High-modulation efficiency silicon Mach-Zehnder optical modulator based on carrier depletion in a PN Diode

Jeong Woo Park, Jong-Bum You, In Gyoo Kim and Gyungock Kim

Electronics and Telecommunications Research Institute
161 Gajeong-dong, Yusong-gu, Daejeon, Republic of Korea
**pjw21@etri.re.kr*

Abstract: We present a high phase-shift efficienct Mach-Zehnder silicon optical modulator based on the carrier-depletion effect in a highly-doped PN diode with a small waveguide cross-sectional area. The fabricated modulator show a $V_\pi L_\pi$ of 1.8V·cm and phase shifter loss of 4.4dB/mm. A device using a 750 μm-long phase-shifter exhibits an eye opening at 12.5Gbps with an extinction ratio of 3 dB. Also, an extinction ratio of 7 dB is achieved at 4 Gbps for a device with a 2 mm-long phase shifter. Further enhancement of the extinction ratio at higher operating speed can be achieved using a travelling-wave electrode design and the optimal doping.

OCIS codes: (250.0250) Optoelectronics; (250.7360) Waveguide modulators; (230.5300) Photonic integrated circuits

References and links

1. R. A. Soref, and B. R. Bennett, "Electrooptical effects in silicon," IEEE J. of Quant. Elec. **23**(1), 123–129 (1987).
2. Q. Xu, B. Schmidt, S. Pradhan, and M. Lipson, "Micrometre-scale silicon electro-optic modulator," Nature **435**(7040), 325–327 (2005).
3. A. Liu, R. Jones, L. Liao, D. Samara-Rubio, D. Rubin, O. Cohen, R. Nicolaescu, and M. Paniccia, "A high-speed silicon optical modulator based on a metal-oxide-semiconductor capacitor," Nature **427**(6975), 615–618 (2004).
4. A. Liu, L. Liao, D. Rubin, H. Nguyen, B. Ciftcioglu, Y. Chetrit, N. Izhaky, and M. Paniccia, "High-speed optical modulation based on carrier depletion in a silicon waveguide," Opt. Express **15**(2), 660–668 (2007).
5. D. Marris-Morini, L. Vivien, J. M. Fédéli, E. Cassan, P. Lyan, and S. Laval, "Low loss and high speed silicon optical modulator based on a lateral carrier depletion structure," Opt. Express **16**(1), 334–339 (2008).
6. A. Huang, C. Gunn, G. Liang, Y. Liang, S. Mirsaidi, A. Narasimha, and T. Pinguet, "A 10Gb/s photonic modulator and WDM MUX/DEMUX integrated with electronics in 0.13mm SOI CMOS", *ISSCC*, 13.7 (2006).
7. G. T. Reed, and A. P. Knights, *Silicon Photonics: an introduction* (John Wiley, Chichester, 2004)

Research interest in silicon optical modulators has been growing. The device's operational schemes are based on a change of refractive index [1] caused by the carrier injection effect in a p-i-n diode [2], the carrier accumulation effect in a MOS capacitor [3], and the carrier depletion effect in a PN diode [4–6]. The carrier-injection-based p-i-n diode modulator suffers from a slow operational speed originating from the slow carrier life time in the intrinsic region without a pre-emphasis driving scheme. This pre-emphasis driver can cause an overhead for on-chip integration of multi-channel input/output (I/O). The MOS capacitor approach shows a high speed operation because of the majority carrier dynamics. However, it requires a high driving power for high-speed operation, and shows a low modulation efficiency. On the other hand, the modulator based on the carrier-depletion effect in a PN diode shows a high-speed operation and can be driven with low power, while it has a low phase-shift efficiency originating from a small overlap between the optical field and active electrical region for a variation of carrier concentration, leading to a low extinction ratio. This drawback in a carrier-depletion PN diode modulator can be improved through an adequate design of the active electrical region. In this report, we have investigated a Mach-Zehnder modulator (MZM) with a highly-doped PN diode, based on a waveguide with a small cross-sectional area.

In order to improve the modulation efficiency of a PN diode MZM, the effects of the optical field confinement within a small area, and the PN junction with a higher doping level

#112277 - $15.00 USD Received 3 Jun 2009; revised 7 Aug 2009; accepted 11 Aug 2009; published 18 Aug 2009

are considered in the device design. Figure 1(a) depicts a schematic cross-sectional view of the phase shifter of a silicon Mach-Zehnder interferometer (MZI). It is comprised of a silicon rib waveguide with a width of 500nm and height of 220nm. Here, the ridge height of the waveguide is about two or three times smaller than in previously reported cases [4,5]. An asymmetric MZI arm is used to simplify the optical characterization. The n-type doping concentration is ~1.0 x 10^{19} cm^{-3}, while the p-type doping concentration are ~1.0 x $10^{18}cm^{-3}$ for a type-(I) modulator, and ~5.0 x 10^{17} cm^{-3} for a type-(II) modulator. To insure good ohmic contact between silicon and metal, the doping concentration of the metal contact region is ~1.0 x $10^{20}cm^{-3}$ for both dopant types. Figure 1(b) shows a micro-photography of the fabricated MZM. Here, a travelling wave electrode was not adopted. A higher doping level can introduce greater change of the carrier concentration in a PN junction interface, which contributes to a more effective index modulation. The confinement of photons and the PN junction interface within a small region lead to a strong overlap between the optical field and the active region of the carrier concentration variation, resulting in an enhancement of the effective index change, and thus leading to a higher extinction ratio.

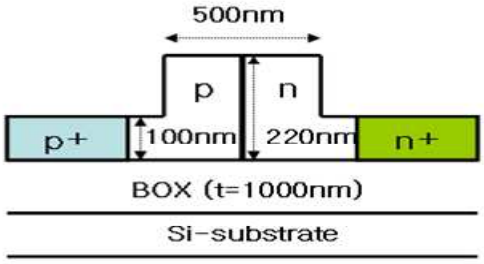

(a)

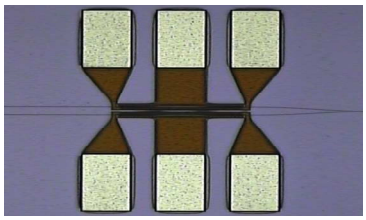

(b)

Fig. 1. (a) Cross-sectional view of a PN junction waveguide phase shifter on a Silicon-On-Insulator (SOI). (b) Micro-photograph of a fabricated MZM

Figure 2(a) shows the measured optical transmission intensity versus applied reverse voltage characteristic of a fabricated type-(I) MZM with a 2 mm-long phase shift arm, which indicates an improvement of phase-shift efficiency using a small cross-sectional area of a rib waveguide and higher doping level. As is shown in the figure, the phase shift due to the carrier depletion effect is measured at up to a −10 V bias, at which the relative phase shift is nearly π. This indicates that the $V_\pi L_\pi$ of the type-(I) device is ~2 V·cm. For a bias of higher than −10 V, an avalanche breakdown occurs, showing that largely the increasing carrier concentration can cause a large phase shift with a small voltage variation.

#112277 - $15.00 USD Received 3 Jun 2009; revised 7 Aug 2009; accepted 11 Aug 2009; published 18 Aug 2009

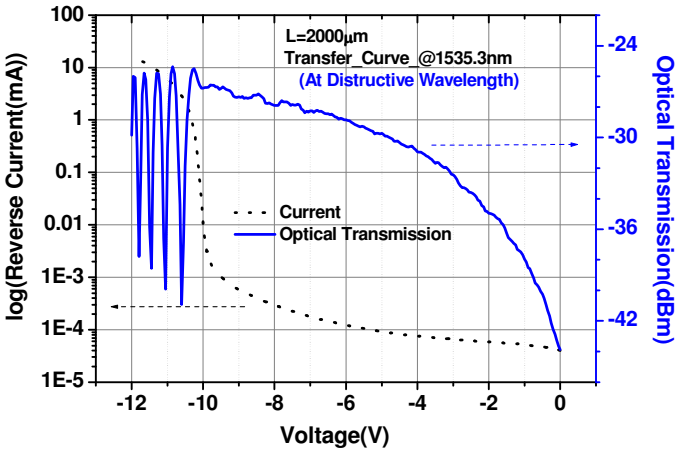

Fig. 2. (a). Optical output intensity of a MZM having a 2mm-long phase shifter versus voltages applied to one of the arms

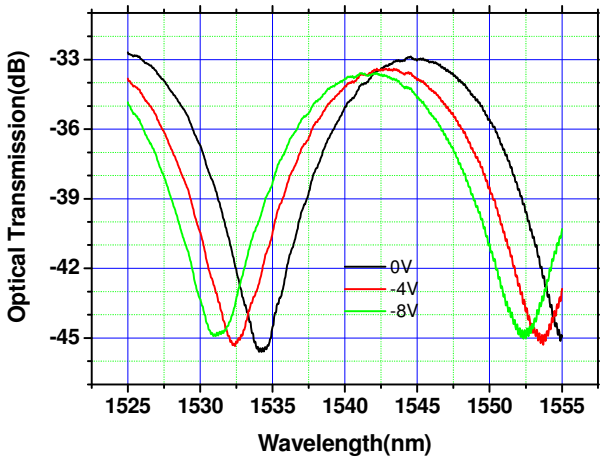

Fig. 2. (b) Output spectra of a MZM having a 1mm-long phase shifter for various voltages applied to one of the arms

Also, a voltage-induced wavelength shift (Δλ) measured in the transmission spectrum of the asymmetric MZI can be used to obtain a voltage-induced phase shift ($\Delta\varphi$) from the relation $\Delta\varphi = 2\pi \cdot \Delta\lambda / FSR$ [4], where FSR is the free spectral range of the asymmetric MZI. As shown in Fig. 2(b), the measured Δλ is 1.93nm with ΔV = 4V, and the measured FSR is 21.3nm for a type-(I) MZM with a 1 mm-long phase shifter. Using the obtained $\Delta\varphi = 0.18\pi$, the figure of merit for the phase shift efficiency, $V_\pi L_\pi$, is also obtained as 1.8 V·cm in a reverse bias range of less than 4V. Type (I) devices show phase shifter loss of 4.4dB/mm. For the type-(II) device with a lower p-type doping level, the measured $V_\pi L_\pi$ was increased to ~3 V·cm, which implies that higher doping can improve the phase-shift efficiency. For the type-(II) device, phase shifter loss was 4dB/mm.

The total on-chip loss for the type-(I) device with a 750 μm-long phase-shift arm was measured as ~7.6 dB when the MZI is on state, where maximum optical transmission occurs.

#112277 - $15.00 USD Received 3 Jun 2009; revised 7 Aug 2009; accepted 11 Aug 2009; published 18 Aug 2009

This on-chip loss includes ~1.5 dB propagation loss of the passive waveguide, ~3.3 dB loss of the phase shifter, and ~2.8 dB loss of the Y-branch splitter/combiner. The phase shifter loss was obtained from a comparison with other modulators that have different phase arm lengths. The propagation loss was measured using the well-known cut back method [7]. The Y-splitter/combiner loss was determined by comparing the loss of MZI with that of a straight reference waveguide.

The high-speed performance of the modulator device has been characterized by measuring both the 3 dB frequency roll-off and the data transmission capability. For the frequency response measurement, the electrical power from a vector network analyzer was applied to one of phase shifters, sweeping the frequency from 50 MHz to more than 10GHz, and a CW laser beam was coupled into the modulator via a lensed fiber. The optical output of the MZM was converted to an electrical signal using a 40 GHz photodiode and the RF frequency spectrum of the converted electrical signal was read using a vector network analyzer. The frequency response of the modulator was obtained by de-embedding the connecting cable/connector response from the total response. Figure 3 shows the measured results for type-(I) device with a 1.5mm-long phase shifter. At a bias of –4 V and with an RF input of –2 dBm, the 3 dB roll-off frequency (f_{3dB}) is measured as ~7 GHz.

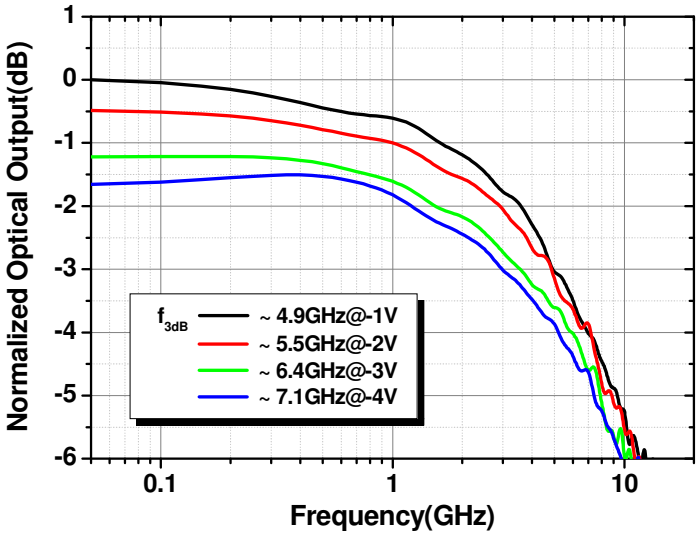

Fig. 3. A frequency spectrum of an optical response as a function of input RF frequency for a MZM [type (I)] having a 1.5mm long phase shift arm.

The data transmission capability of the fabricated device was characterized by measuring the eye-pattern. A signal from a pseudo-random bit sequence (PRBS) generator is amplified using a commercially available RF amplifier. An amplified output signal of V_{pp} = 4V is combined with a –4 V DC bias using a bias-tee. The pattern length of the signal from the PRBS is 2^7-1. Figure 4 shows the on-chip measurement of the optical eye diagrams at a bit rate of 12.5Gbps for the device with a 750μm-long phase shifter. The measured extinction ratio is ~3dB, indicating improved values compared to previous results in a PN-diode based silicon modulator.

#112277 - $15.00 USD Received 3 Jun 2009; revised 7 Aug 2009; accepted 11 Aug 2009; published 18 Aug 2009

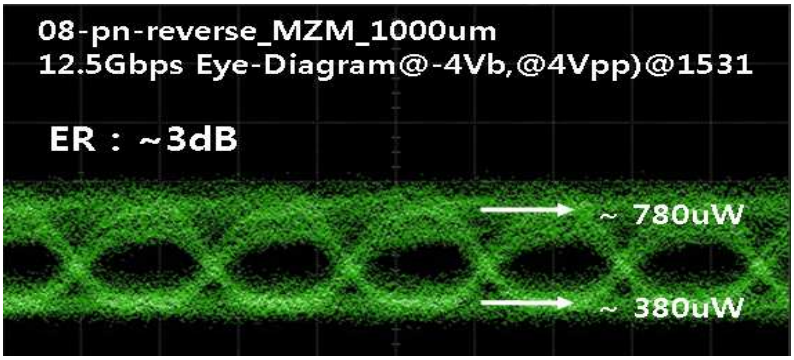

Fig. 4. An eye diagram of a MZM [type(I)] with a 750μm-long phase shift arm at a bit rate of 12.5Gbps

Further improvement of the extinction ratio is possible using a device with a longer phase shifter. Figure 5 shows an eye diagram of a 2 mm-long phase-shifter device at a bit rate of 4 Gbps. It exhibits a high extinction ratio of ~7 dB. However, the operating speed is limited by its capacitance, and this limit can be overcome using a travelling wave electrode design.

Using the optimum doping and travelling wave electrode design, further improvement of the extinction ratio at a higher speed operation can be achieved.

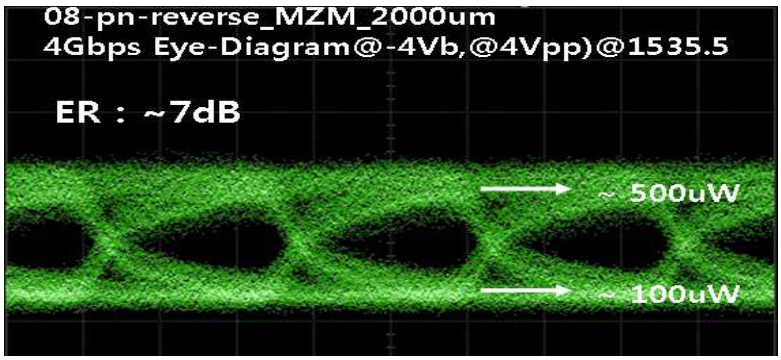

Fig. 5. A measured eye diagram of the a type-(I) MZM with 2mm-long phase arm, showing a ~7 dB extinction ratio at a bit rate of 4Gbps.

In conclusion, the effect of the high doping concentration in a PN diode with a smaller cross-sectional area rib waveguide has been investigated in a carrier-depletion PN-diode Mach-Zehnder silicon modulator. The measured phase-shift efficiency of the fabricated modulator, $V_\pi L_\pi$, is 1.8 V·cm, indicating a high phase-shift efficiency. The device with a 1.5 mm-long phase shifter shows a 3-dB bandwidth of 7 GHz. The extinction ratio of 3 dB at a bit rate of 12.5Gbps is obtained in a device with a 750 μm-long phase-shifter, showing an enhanced extinction ratio. Also the device with a 2 mm-long phase shifter exhibits a high extinction ratio of ~7 dB at a bit rate of 4 Gbps. With the addition of a travelling wave electrode and optimum doping design, further improvement of the extinction ratio and the operating speed of the modulator can be possible.

#112277 - $15.00 USD Received 3 Jun 2009; revised 7 Aug 2009; accepted 11 Aug 2009; published 18 Aug 2009